

Figure S1, related to Figure 2: Plasma and insulin concentrations during clamp. Plasma glucose (Pre: closed circle; Post: open square) and insulin (Pre: closed square; post: open triangle) in young participants before and after high-intensity interval training (HIIT, panel A), resistance training (RT, panel B) combined training (CT, panel C) or sedentary period (SED, panel D). Shaded region represents target glucose at 85-95 mg/dl. Data displayed as mean±SEM.

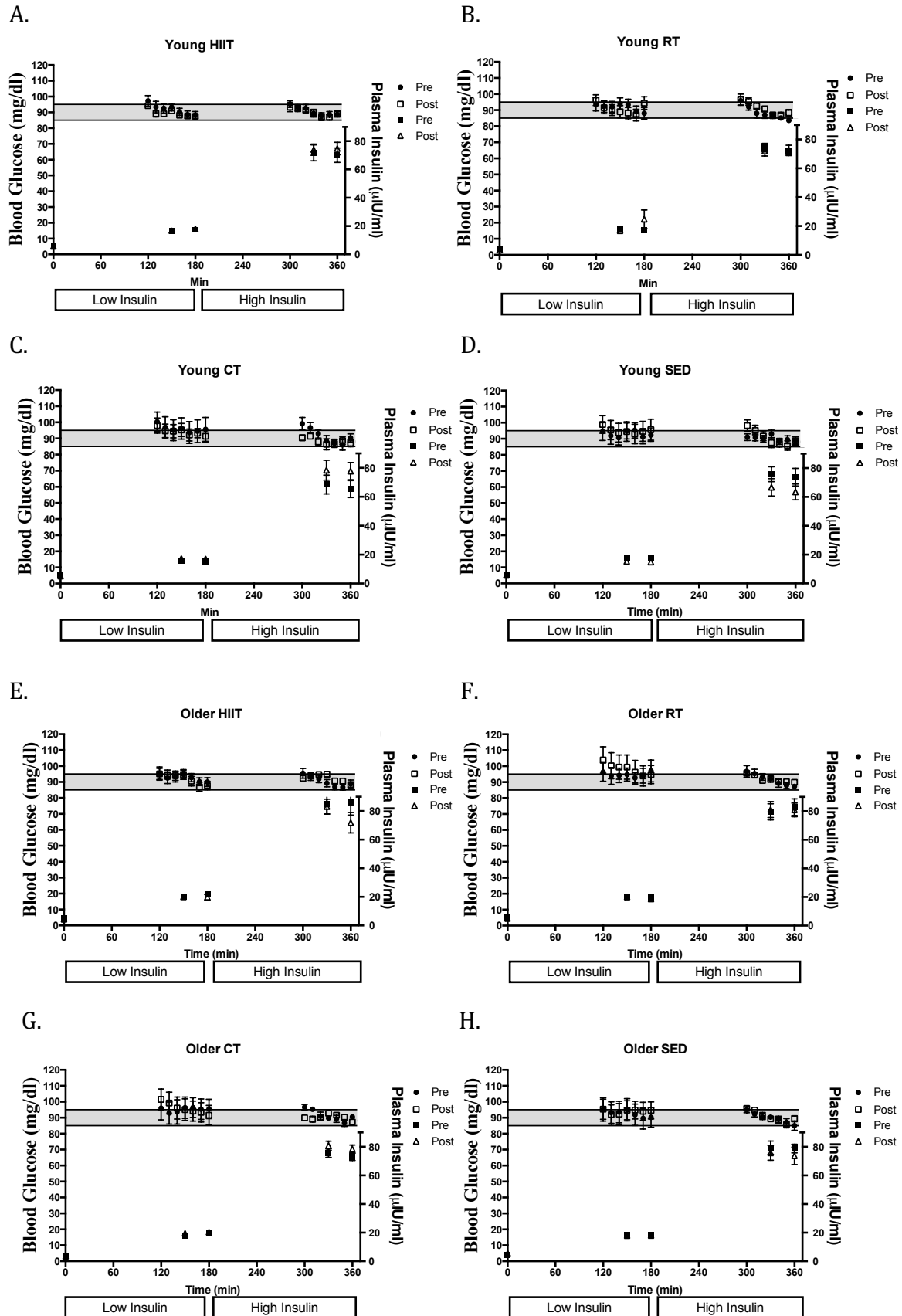


Figure S2, related to Figure 2: Plasma tracer enrichment during clamp. Plasma [6,6]-H₂ glucose enrichment during basal, low and high insulin infusion. Data displayed as mean±SD.

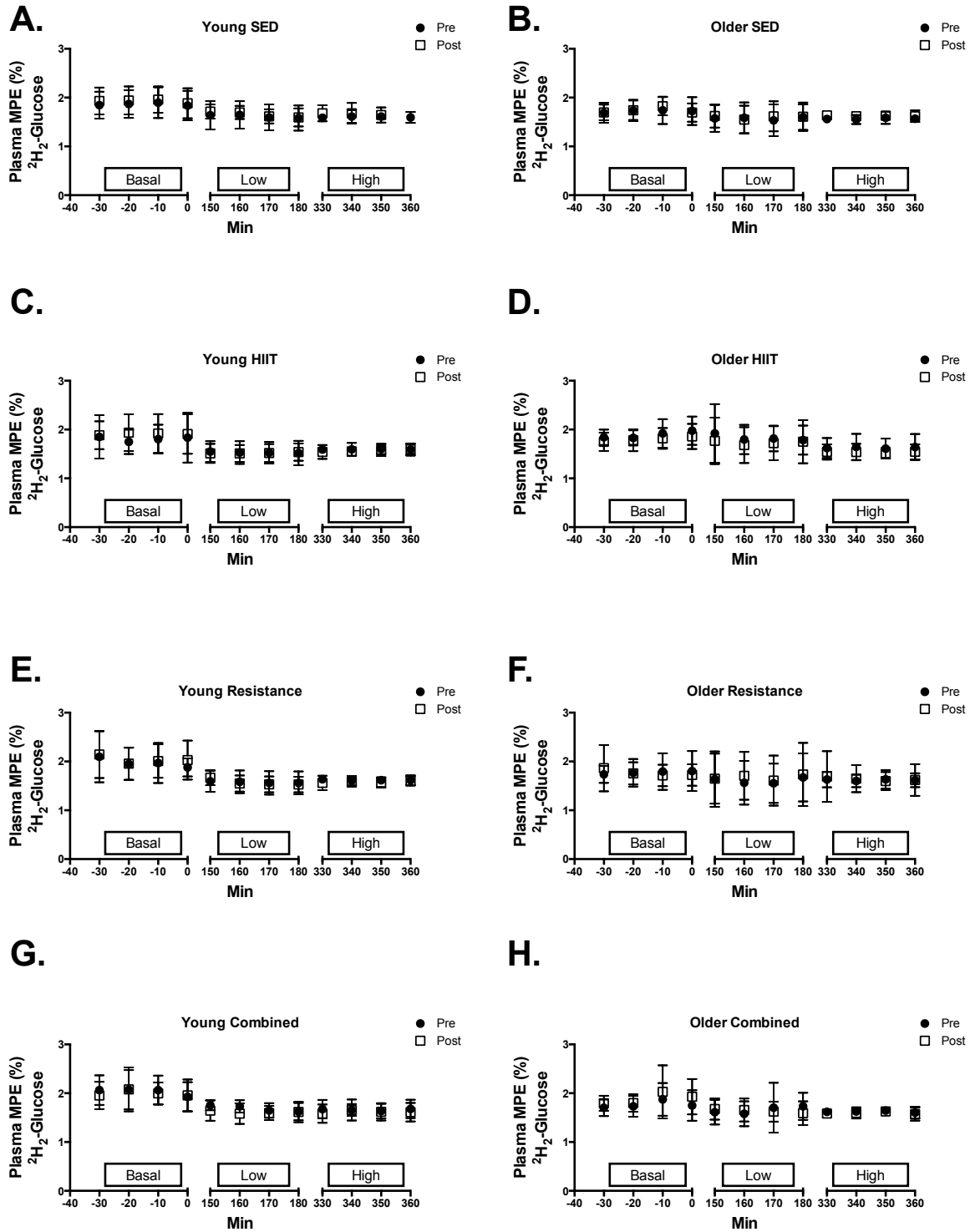


Figure S3, related to Figure 2: Endogenous glucose production (EGP) per kg lean mass during Basal, Low and High insulin euglycemic clamp stages in young (A) and older (B). Carbohydrate metabolism was measured using $^2\text{H}_2$ -glucose and indirect calorimetry revealing similar rates of glucose disappearance (R_d) through oxidative and non-oxidative pathways at baseline (C). The increased glucose R_d with training occurred predominantly through increases in non-oxidative glucose disposal, primarily representing glycogen storage (D). Data are displayed as mean \pm SD. Measurements were performed before and after 12 weeks of high-intensity interval training (HIIT), resistance training (RT) combined training (CT) or sedentary period (SED).

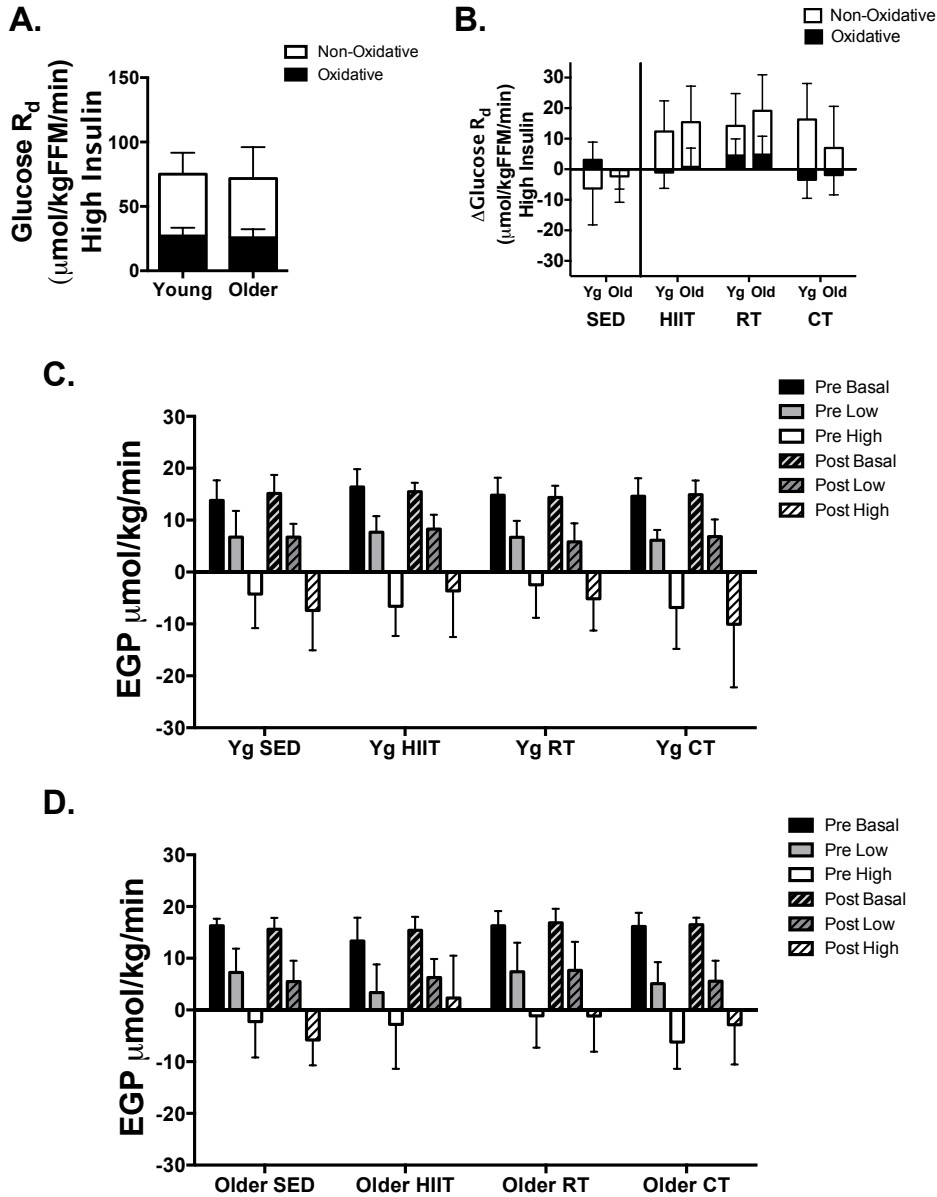


Figure S4, related to Figure 3: Respiratory control ratio, H₂O₂ production and mtDNA content.

Mitochondrial respiratory control ratio (RCR) measured using high-resolution respirometry during State 3 respiration of substrates for CI and II (Glutamate+Malate+Succinate+ADP) and leak state induced by oligomycin (Leak_{Oligo}) at baseline (A) and following 12 weeks of training (B). Mitochondrial H₂O₂ production normalized to mitochondrial protein content was similar at baseline (C) and did not change with 12 weeks of exercise training (D). The ratio of mitochondrial DNA (mtDNA) to nuclear DNA was measured by qPCR and was lower at baseline in older adults (E), then increased in older adults (F) following 12 weeks of high-intensity interval training (HIIT), resistance training (RT) and combined training (CT). There was a high correlation between Pre and Post testing for peak aerobic capacity (VO_{2 peak}) in the sedentary control group (G). Changes during SED were analyzed separately and included in graphs for comparison. Data from baseline comparisons are displayed as Mean±SD with p-values for un-paired t-test. Changes with training are presented as least square adjusted mean with Tukey HSD 95% confidence intervals. Non-overlapping confidence intervals are different at the corrected α level. Dotted line is set at zero (no change from baseline). *p<0.05 for old versus young.

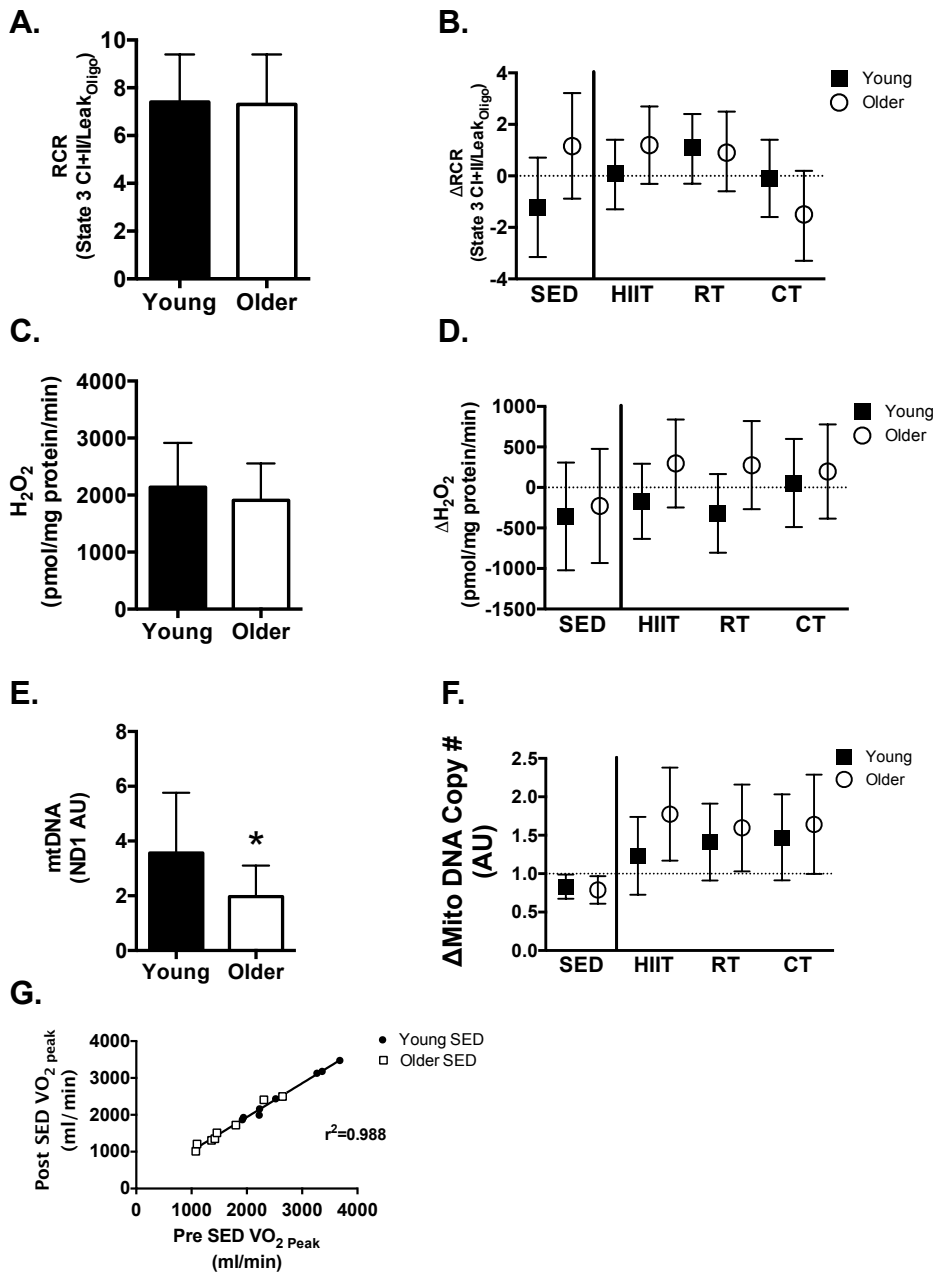
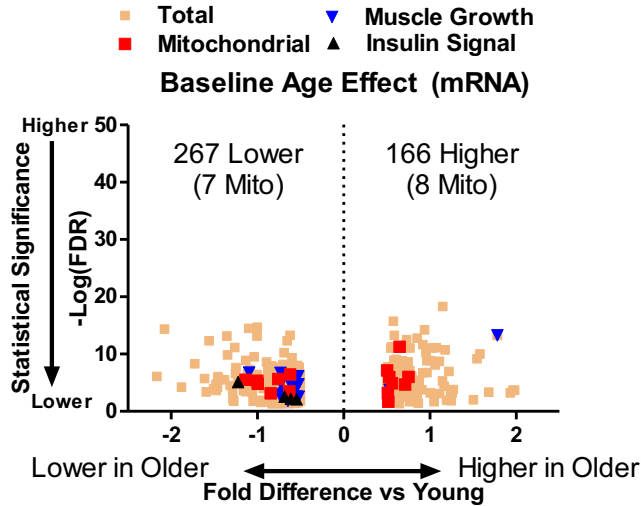


Figure S5, related to Figure 4: Gene expression between age groups and after training. (A) Genes that are differentially expressed between young and old, at baseline, were detected by using an adjusted p-value of ≤ 0.05 and an absolute fold change of ≥ 0.5 . Genes were annotated according to their mitochondrial specificity (using MitoCarta) and molecular function (using KEGG). Mito stands for mitochondrial. (B) Gene set enrichment analysis of baseline gene expression differences between young and old subjects against genes that were up regulated with HIIT in younger subjects is shown below. Genes that increased expression with age are more likely increase their expression with HIIT in younger subjects.

A.



B.

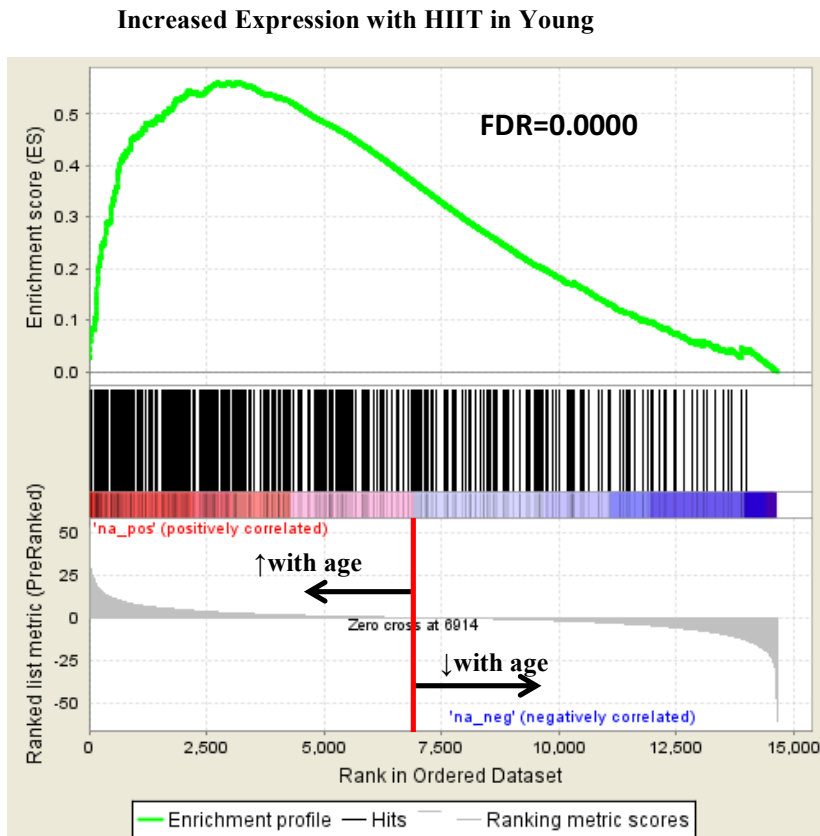
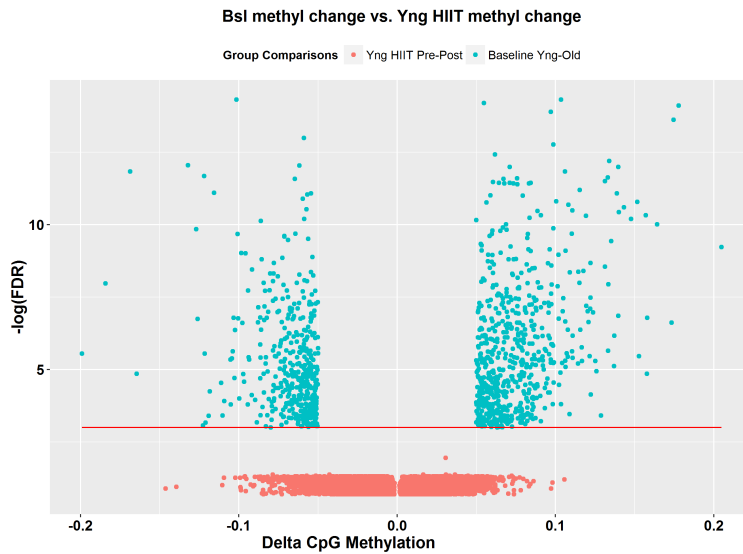


Figure S6, related to Figure 4: Promoter CpG methylation is not affected by exercise training. Skeletal muscle biopsies were analyzed using Illumina 450K methylation array. GenomeStudio software processed the data to remove background and normalize signal to account of technical variation. Partek software analyzed the processed CpG data. Site-level CpG methylation (β) values were used to compute differential methylation p-values and delta methylation change between two groups. Computed p-values were corrected using Benjamini-Hochberg method. CpG sites that were within promoter regions (defined as $2000\text{bp} \leq \text{TSS} \leq 500\text{bp}$) were considered for further analysis. Panels show the FDR and Δ values of promoter CpGs that were differentially expressed (defined as $\text{FDR} \leq 0.05$ and absolute $\Delta\beta \geq 0.05$ between young vs. old (in blue color) at baseline. For exercise training, $\Delta\beta$ was computed as Pre-exercise training minus Post-exercise training. Example data from Young (A) and Older HIIT (B) show the exercise training induced $\Delta\beta$ and FDR values associated with promoter CpGs (in red). Red horizontal line in the panels correspond to $\text{FDR} \leq 0.05$ threshold. We did not observe significant changes in methylation of promoter CpGs with any type of exercise modality.

A.



B.

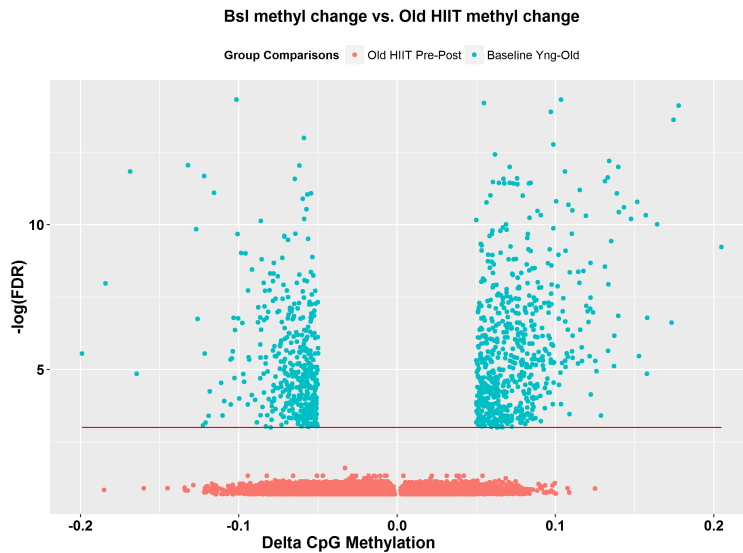


Table S1, related to Figure 4: This table shows genes that had a statistically significant decrease in expression with age as well as statistically significant increase in expression with HIIT in older subjects. Gene expression data of young and old subjects at baseline was used to derive a set of genes that changed expression with age. Gene expression data of post- and pre-HIIT samples collected from older subjects was used to detect genes that changed expression with HIIT. Both lists were filtered to retain only genes with an adjusted p-value ≤ 0.05 and at least an absolute fold change of ≥ 0.5 . The method is described in greater detail in the methods section of the study. Genes that went up with age also had a higher change to go up with physical activity in older subjects. * "up-up" means that the gene's expression increased with age and HIIT. "down-up" means that the gene's expression decreased with age and increased with HIIT.

Gene	Baseline Old vs. Young		Old HIIT Pre vs. Post		Change Interpretation*
	Log2(Fold Change)	FDR	Log2(Fold Change)	FDR	
IGF2	0.573225577	2.73E-06	0.860981461	2.6105E-11	up-up
ELN	0.845097465	0.000700318	0.859524056	1.53209E-07	up-up
PTPRC	0.612853682	0.004924745	0.830512358	0.00126463	up-up
AC132217.4	0.504441162	6.16E-05	0.816010314	7.83098E-10	up-up
INS-IGF2	0.663745361	3.56E-07	0.802602631	5.21645E-10	up-up
LAPTM5	0.536464347	0.002708274	0.781841327	0.000121204	up-up
LYZ	0.642874452	0.016727124	0.765799265	0.018607754	up-up
ITGB2	0.686089398	0.001140919	0.746669634	2.7138E-05	up-up
POSTN	1.139298138	0.000262533	0.743662601	0.003101744	up-up
CTSS	0.529063288	0.001447605	0.729192133	0.005030352	up-up
COL14A1	0.628259085	0.005614664	0.719181437	0.002396621	up-up
PLVAP	0.584887234	0.000170106	0.704998152	2.29907E-07	up-up
CCL15-CCL14	0.760680639	0.000191943	0.645393409	7.84269E-06	up-up
LUM	0.707076636	6.00E-06	0.63843606	4.69192E-05	up-up
CCL14	0.778072652	0.000146586	0.635797524	2.89738E-05	up-up
C1QA	0.728285516	0.000297163	0.622780551	0.000525376	up-up
RP11-475J5.5	0.846631514	0.007335166	0.607245373	0.00024757	up-up
MS4A6A	0.604126451	0.000938859	0.568254916	0.003459616	up-up
SULF1	0.756460344	0.00020251	0.532929432	0.003041846	up-up
SVEP1	0.516246704	7.20E-05	0.528584541	1.21371E-06	up-up
CD68	0.585070646	7.45E-05	0.522973162	0.005329399	up-up
STAB1	0.601861305	2.07E-05	0.515764604	5.10974E-06	up-up
METTL21EP	-1.544862436	6.80E-10	1.149941483	5.42431E-20	down-up
MYLK4	-1.7816154	5.35E-14	0.987422649	6.26132E-06	down-up
SCN4B	-0.728624604	1.63E-06	0.832109883	8.82236E-12	down-up
PKP1	-0.505637978	0.016918581	0.825261225	9.81716E-08	down-up
MT-TR	-0.711199107	2.02E-05	0.809985436	2.71365E-24	down-up
RP11-296E23.1	-0.637033435	0.01146624	0.724176323	1.41583E-12	down-up
MTRNR2L6	-0.5874597	0.007294797	0.66503461	2.03776E-08	down-up
AC009234.1	-0.765398424	0.020402689	0.620189476	1.94449E-09	down-up
KAZALD1	-0.675924682	0.001985578	0.602525638	0.00957209	down-up
RP11-61I13.3	-0.966345784	1.74E-07	0.530722984	0.000671561	down-up
CKMT2	-0.530069962	1.03E-06	0.527590589	8.13471E-06	down-up

Table S2, related to Figure 4: Genes that were universally upregulated with exercise training regardless of age and modality are shown here. FC stands for fold change. FDR stands for false discovery rate which was calculated with Benjamini-Hochberg adjusted p-values of mRNA differential expression. A $\log_2(\text{FC})$ of ≥ 0.3 and an $\text{FDR} \leq 0.05$ were applied to generate the list. $\log_2(\text{FC})$ was relaxed from 0.5 in order to increase the likelihood to detect genes whose expression changed by a small degree and yet consistently across all age groups and modalities. These genes were used for pathway analysis by Ingenuity Pathways (IPA, Qiagen, Germany).

Gene Symbol	Young Combined		Young Resistance		Young HIIT		Old Combined		Old Resistance		Old HIIT	
	$\log_2(\text{FC})$	FDR	$\log_2(\text{FC})$	FDR	$\log_2(\text{FC})$	FDR	$\log_2(\text{FC})$	FDR	$\log_2(\text{FC})$	FDR	$\log_2(\text{FC})$	FDR
CD34	0.508	2.96E-02	0.411	4.19E-04	0.329	3.43E-02	0.437	3.66E-04	0.326	6.10E-03	0.570	2.51E-09
EFNA1	0.731	3.08E-03	0.556	8.06E-04	0.426	4.05E-02	0.549	4.45E-02	0.687	1.88E-03	0.925	2.62E-17
NID1	0.637	8.19E-04	0.605	2.14E-11	0.686	2.00E-05	0.637	1.34E-06	0.655	4.01E-10	1.035	3.57E-38
NPR1	0.689	8.39E-05	0.726	3.49E-06	0.617	3.60E-03	0.625	2.57E-03	0.574	5.10E-03	1.033	5.77E-12
TIE1	0.854	3.97E-07	0.699	3.47E-05	0.406	3.60E-02	0.455	6.23E-03	0.593	7.35E-04	0.961	6.41E-16
UNC5B	0.626	2.79E-02	0.881	1.53E-06	0.668	1.94E-03	0.749	5.91E-05	1.005	1.36E-07	1.330	5.44E-19
AC132217.4	0.635	3.83E-03	0.814	7.19E-08	0.499	7.75E-03	0.474	4.84E-02	0.629	3.01E-05	0.816	7.83E-10
ETS1	0.592	3.30E-03	0.607	1.06E-06	0.399	9.82E-03	0.565	9.54E-06	0.390	1.92E-03	0.721	1.03E-15
A2M	0.661	6.47E-04	0.506	1.46E-06	0.360	4.34E-02	0.399	8.04E-03	0.398	3.84E-03	0.680	1.73E-09
ELK3	0.629	8.97E-03	0.572	5.75E-07	0.470	2.53E-03	0.469	9.63E-04	0.508	2.62E-04	0.724	4.69E-13
KCNJ8	0.716	1.44E-03	0.542	1.76E-03	0.413	3.51E-02	0.543	5.34E-03	0.533	5.31E-06	0.992	1.33E-17
KITLG	0.584	1.09E-03	0.554	3.24E-05	0.320	4.26E-02	0.443	3.37E-02	0.363	1.01E-02	0.386	6.57E-04
OAS2	0.704	5.49E-03	0.782	2.04E-07	0.879	9.18E-03	0.670	1.60E-03	0.653	3.25E-04	1.343	1.34E-06
COL4A1	0.887	7.39E-05	1.418	3.56E-25	1.118	2.28E-06	0.975	1.34E-06	1.237	1.59E-31	1.855	5.17E-43
COL4A2	0.779	2.57E-03	1.132	6.87E-19	0.912	8.48E-05	0.861	2.82E-05	1.013	3.33E-21	1.601	9.12E-42
EDNRB	1.086	5.15E-05	1.168	1.28E-18	0.947	4.69E-05	1.187	5.80E-12	0.965	3.11E-04	1.704	1.37E-19
LPAR6	0.588	4.51E-02	0.519	5.54E-05	0.581	1.85E-03	0.612	5.34E-03	0.367	1.51E-02	0.839	1.34E-12
RNASE1	0.482	2.27E-03	0.537	2.33E-06	0.389	9.94E-03	0.398	8.92E-04	0.527	7.18E-06	0.635	2.17E-13
CDH5	0.686	5.08E-05	0.657	5.10E-09	0.478	5.79E-03	0.393	3.29E-03	0.551	6.92E-06	0.949	8.23E-22
ACE	0.534	1.21E-02	0.598	3.90E-05	0.430	3.14E-02	0.550	1.29E-03	0.484	3.00E-03	0.707	4.10E-10
BCL6B	0.592	1.89E-02	0.829	1.87E-07	0.582	1.94E-02	0.740	2.72E-04	0.843	1.29E-06	1.071	1.54E-16
CD300LG	1.044	3.98E-12	0.822	7.19E-08	0.638	1.18E-02	0.918	1.75E-11	0.809	1.97E-07	1.364	1.29E-18
RNF152	0.718	3.44E-02	0.578	2.12E-06	0.604	1.30E-02	0.660	2.25E-03	0.777	6.40E-07	1.282	1.17E-31
HECW2	0.834	3.72E-03	0.468	3.50E-04	0.563	6.55E-03	0.892	1.29E-05	0.710	9.15E-03	1.008	6.19E-08
ID2	0.693	3.02E-02	0.390	2.96E-02	1.102	5.35E-05	0.722	3.09E-03	0.935	5.33E-04	0.795	3.07E-07
MYO1B	0.617	3.77E-03	0.599	2.72E-07	0.425	5.04E-03	0.543	2.06E-03	0.564	3.67E-06	0.907	7.40E-12

PXDN	0.692	8.45E-04	1.227	3.94E-23	0.971	2.99E-06	0.734	3.75E-03	1.064	6.31E-20	1.413	2.99E-36
CD93	0.678	5.82E-05	0.800	5.69E-10	0.528	3.05E-03	0.559	1.37E-03	0.596	2.13E-07	0.957	5.44E-19
EPB41L1	0.590	7.98E-04	0.485	4.19E-06	0.390	1.37E-02	0.381	7.10E-03	0.327	2.79E-02	0.562	1.42E-09
JAM2	0.684	3.09E-03	0.442	1.12E-03	0.467	1.20E-02	0.551	2.01E-03	0.580	1.05E-05	0.899	5.75E-11
ARHGAP31	0.597	4.77E-04	0.522	1.88E-04	0.396	1.66E-02	0.406	1.86E-02	0.426	1.57E-02	0.776	1.15E-11
MECOM	0.763	2.91E-06	0.785	3.59E-07	0.518	2.94E-02	0.512	2.03E-02	0.566	5.95E-03	1.053	8.23E-22
PLXND1	0.424	1.02E-02	0.581	1.26E-05	0.456	3.53E-03	0.345	2.13E-02	0.369	6.43E-03	0.693	4.88E-13
TM4SF18	0.778	3.59E-03	0.824	1.24E-08	0.824	8.97E-07	0.684	3.09E-03	0.575	1.34E-03	0.993	1.34E-18
GUCY1A3	0.585	7.22E-03	0.508	4.62E-05	0.377	1.26E-02	0.377	3.00E-02	0.455	1.93E-03	0.630	5.33E-07
BTNL9	1.085	2.79E-07	0.632	6.09E-06	0.626	9.28E-03	0.843	4.58E-18	0.574	1.31E-02	1.116	9.38E-21
F2R	0.868	6.24E-03	0.817	7.15E-07	0.946	2.33E-05	0.568	2.93E-02	0.865	3.00E-07	1.133	2.49E-16
PCDH12	0.791	1.24E-03	0.772	1.87E-06	0.557	8.36E-03	0.643	5.34E-03	0.817	1.37E-04	1.061	7.19E-13
PDGFRB	0.493	2.71E-02	0.511	2.05E-08	0.451	1.71E-03	0.379	1.52E-02	0.476	1.34E-06	0.722	1.24E-14
SPARC	0.486	2.99E-02	0.769	1.05E-11	0.907	1.85E-07	0.719	3.66E-04	0.841	1.24E-08	1.162	2.57E-34
GJA1	0.646	3.59E-03	0.861	1.35E-15	0.674	6.45E-04	0.418	2.33E-02	0.407	1.49E-02	0.799	5.76E-12
NOTCH4	0.644	1.38E-04	0.696	5.82E-06	0.474	1.62E-02	0.499	2.18E-02	0.419	4.90E-02	0.890	4.87E-18
SH3BGRL2	0.809	8.61E-05	0.451	4.42E-03	0.514	5.31E-03	0.489	2.17E-02	0.377	2.16E-02	0.777	1.10E-09
CAV1	0.652	4.63E-04	0.535	2.27E-05	0.352	2.60E-02	0.393	1.66E-02	0.403	2.40E-03	0.742	7.88E-13
CDK6	0.435	4.11E-02	0.746	5.10E-09	0.581	1.91E-03	0.506	1.54E-02	0.578	2.38E-04	0.831	1.52E-10
GNG11	0.754	1.49E-05	0.625	5.23E-09	0.419	3.64E-02	0.599	3.23E-04	0.390	7.15E-04	0.868	3.27E-18
LAMB1	0.576	2.65E-03	0.624	1.07E-11	0.772	7.14E-08	0.679	1.67E-09	0.440	2.06E-03	0.763	5.20E-11
RAPGEF5	0.816	6.75E-04	0.875	4.47E-09	0.587	3.21E-03	0.705	1.06E-04	0.470	4.28E-03	0.808	2.37E-09
C8orf4	0.923	2.00E-06	0.608	6.35E-06	0.540	3.01E-02	0.892	2.55E-06	0.770	3.28E-06	1.119	1.68E-13
ASPN	0.656	7.47E-03	0.902	4.30E-06	0.801	1.19E-03	0.822	1.30E-03	1.281	3.66E-11	1.214	7.27E-19
ECM2	0.497	1.28E-02	0.689	3.20E-05	0.805	6.75E-06	0.534	5.93E-03	0.793	1.29E-06	0.844	1.12E-10
S1PR3	1.082	4.60E-04	1.102	7.39E-08	0.794	1.86E-04	0.786	9.63E-04	0.679	1.81E-04	1.086	9.29E-07
ITM2A	0.373	3.15E-02	0.386	4.67E-06	0.398	2.96E-03	0.433	7.71E-03	0.447	5.19E-04	0.577	5.47E-08
PLS3	0.545	4.51E-03	0.421	6.35E-06	0.405	2.34E-03	0.465	3.85E-04	0.515	2.98E-06	0.664	1.98E-09
TMSB4X	0.545	4.67E-04	0.541	5.07E-07	0.406	5.02E-03	0.404	1.49E-02	0.379	5.88E-04	0.780	5.43E-16

Table S3, related to Figure 4: This table shows the top two Gene Ontology Processes that were enriched when using the 55 genes that were universally upregulated with exercise training, regardless of age and training modality (listed in **Supplemental Table S4**). MetaCore software (Thomson Reuters, New York, NY) was used for the analysis.

Name	FDR	In Data	Target molecules in the data set
angiogenesis	4.158E-15	20	ETS, Ephrin-A, ACE1, NOTCH4, Ephrin-A1, PDGF-R-beta, UNC5B, Plexin D1, Notch, ETS1, PDGF receptor, Galpha(q)-specific peptide GPCRs, COL4A2, Caveolin-1, TIE, COL4A1, Galpha(i)-specific EDG GPCRs, Collagen IV, Elk-3, CD34
regulation of angiogenesis	6.360E-13	16	Guanylate cyclase A (NPR1), ETS, Ephrin-A, NOTCH4, Ephrin-A1, Galpha(s)-specific nucleotide-like GPCRs, Plexin D1, Notch, ETS1, Guanylate cyclase, Galpha(q)-specific peptide GPCRs, COL4A2, Osteonectin, TIE, Collagen IV, CD34

Table S4, related to Figure 4: This table shows the top up stream regulators of the 55 genes that were universally up-regulated with exercise training, regardless of age and training modality. Ingenuity Pathway Analysis software (Qiagen, Germany) was used for the analysis. A p-value threshold of ≤ 0.05 was used to derive the list.

Upstream Regulator	Molecule Type	Predicted Activation State	Activation z-score	p-value of overlap	Target molecules in the dataset
VEGFA	growth factor	Activated	2.069	1.15E-11	ACE,BCL6B,CAV1,CD34,CDH5,ETS1,GJA1,NOTCH4,SPARC,TMSB10/TMSB4X,UNC5B
Vegf	group	Activated	3.095	1.76E-07	A2M,ACE,CD93,CDH5,EFNA1,ETS1,JAM2,KITLG,LPAR6,NOTCH4
AGT	growth factor	Activated	2.419	7.20E-07	ACE,CAV1,COL4A1,EDNRB,ETS1,GJA1,KITLG,LAMB1,NOTCH4
FGFR2	kinase	Activated	2	9.66E-06	COL4A1,COL4A2,GJA1,ID2,LAMB1
CTNNB1	transcription regulator	Activated	2.607	2.33E-05	CD34,COL4A1,COL4A2,F2R,GJA1,ID2,LAMB1,MECOM,PLS3
SP1	transcription regulator	Activated	2.392	3.01E-05	CAV1,CDK6,F2R,GJA1,JAM2,NPR1,PDGFRB,SPARC
IL10RA	transmembrane receptor	Activated	2.449	8.01E-05	ASPN,CD34,EDNRB,KITLG,MECOM,SPARC

Table S5, related to Figure 5: This table shows the top pathways that were enriched for proteins that were upregulated with HIIT and resistance training regimens in old cohort. Up regulated proteins that are associated with each enriched pathway is also listed. MetaCore software (Thomson Reuters, New York, NY) and WEBGESTALT software were used for the analysis.

Pathway	FDR	# Genes	Genes
Older HIIT			
Electron transport chain	1.16E-47	34	ATP5B, ATP5C1, ATP5D, ATP5F1, ATP5H, ATP5J, ATP5S, COX17, COX4I1, COX5A, COX5B, COX6B1, COX6C, NDUFA10, NDUFA2, NDUFA5, NDUFA9, NDUFB10, NDUFB3, NDUFB4, NDUFB6, NDUFB9, NDUFS2, NDUFS4, NDUFS5, NDUFS8, NDUFV2, SLC25A4, SURF1, UCP3, UQCRC1, UQCRC2, UQCRFS1, UQCRH
Oxidative phosphorylation	2.79E-26	19	ATP5B, ATP5D, ATP5F1, ATP5H, ATP5J, ATP5S, NDUFA10, NDUFA2, NDUFA5, NDUFA9, NDUFB10, NDUFB4, NDUFB6, NDUFB9, NDUFS2, NDUFS4, NDUFS5, NDUFS8, NDUFV2,
TCA cycle	3.40E-12	8	DLST, IDH2, IDH3A, IDH3B, IDH3G, MDH2, SUCLA2, SUCLG1
Glycolysis and Gluconeogenesis	2.00E-04	5	GOT1, GOT2, MDH2, MPC2, PDHA1
Branched-chain amino acid catabolism	1.83E-08	6	ACAD8, AUH, HIBADH, HIBCH, HSD17B10, IVD
tRNA aminoacylation	1.93E-07	7	IARS, IARS2, LARS, LARS2, PPA2, WARS2, YARS2
Older Resistance Training			
tRNA Aminoacylation	1.08E-16	12	AARS, AIMP2, DARS, GARS, HARS, IARS, LARS, LARS2, NARS, QARS, SARS, SARS2 CTNNA1, CTNNB1, CTTN, CUL1, DYNLRB1, EXOC1, EXOC4, HK1, HSPA4, HSPA8, HSPD1, INPPL1, NDUFAF2, PPP2CB, PPP5C, RUVBL2, SERPINB5, SLC2A1, TMEM126A, TRIM28, USP7
Insulin Pathway	2.77E-06	21	
TCA cycle	1.44E-02	2	IDH3A, IDH3B
Valine, leucine, and isoleucine biosynthesis	1.00E-04	3	LARS, IARS, LARS2

Table S6, related to Figure 6: This table shows GSEA enrichment results of HIIT-induced muscle proteome changes in older individuals. Differential expression p-value and fold change (FC) between post-HIIT and pre-HIIT samples in older individuals were computed as described in the methods. Protein accessions were converted to gene names. Genes were ranked based on the decreasing order of $-1 * \text{sign}(\text{FC}) * \log_2(\text{FDR adjusted differential P-value})$. GSEA software was used to configure to search the MSigDB for enriched gene sets using the ranked protein list. Gene sets with an adjusted q-value of ≤ 0.05 were listed above. ES stands for enrichment score. NES stands for normalized enrichment score. FDR q-value was computed by using 1000 random permutations of the gene set.

MSigDB NAME	SIZE	ES	NES	FDR q-val
REACTOME_TCA_CYCLE_AND_RESPIRATORY_ELECTRON_TRANSPORT	98	0.80670726	1.6402091	0.015359001
MITOCHONDRIAL_MEMBRANE_PART	37	0.8358765	1.643043	0.015876135
MITOCHONDRIAL_PART	98	0.8013573	1.6335788	0.016824273
MITOCHONDRIAL_INNER_MEMBRANE	44	0.82584995	1.6446171	0.01856849
MITOCHONDRIAL_ENVELOPE	64	0.8213732	1.6453375	0.023904275
REACTOME_BRANCHED_CHAIN_AMINO_ACID_CATABOLISM	16	0.84954023	1.6063995	0.024836736
KEGG_OXIDATIVE_PHOSPHORYLATION	74	0.7972609	1.6082413	0.02569602
REACTOME_RESPIRATORY_ELECTRON_TRANSPORT_ATP_SYNTHESIS_BY_CHEMIOSMOTIC_COUPLING_AND_HEAT_PRODUCTION_BY_UNCOUPLING_PROTEINS	65	0.80456537	1.614258	0.028167063
ORGANELLE_INNER_MEMBRANE	46	0.8238658	1.650944	0.030729769
REACTOME_RESPIRATORY_ELECTRON_TRANSPORT_ENVELOPE	53	0.79198813	1.5957903	0.031386584
MITOCHONDRION_ORGANIZATION_AND_BIOGENESIS	94	0.7735709	1.5799711	0.036652796
ORGANELLE_ENVELOPE	26	0.8183807	1.5822403	0.037440244
REACTOME_PYRUVATE_METABOLISM_AND_CITRIC_ACID_TCA_CYCLE	94	0.7735709	1.574672	0.039162777
MITOCHONDRION	37	0.7918554	1.5834688	0.03953332
MITOCHONDRIAL_MEMBRANE	217	0.77007204	1.5699617	0.041331954
MITOCHONDRIAL_RESPIRATORY_CHAIN	57	0.82512456	1.6592821	0.042696852
REACTOME_CITRIC_ACID_CYCLE_TCA_CYCLE	19	0.82958716	1.5651703	0.0432108
REACTOME_CITRIC_ACID_CYCLE_TCA_CYCLE	19	0.8183239	1.5543818	0.049609795

Table S7, related to Figure 6: Ribosomal proteins were up regulated with high-intensity interval training (HIIT) and resistance training (RT) in older subjects. Differential expression p-value and fold change (FC) between post-HIIT and pre-HIIT samples in older individuals were computed as described in the methods. Protein accessions were converted to gene names. FDR stands for false discovery rate, which was computed using Benjamini-Hochberg method. Mitochondrial ribosomal proteins that play a role in mitochondrial protein synthesis were up regulated with HIIT and RT in older subjects.

Accession	Symbol	Entrez Gene Name	Log FC [Post-Pre]	P-value	FDR
Older HIIT					
NP_001186780.1	MRPS29	28S ribosomal protein S29 mitochondrial assembly of ribosomal large subunit 1	2.133979418	2.24E-10	1.26E-07
NP_612455.1	MALSU1	mitochondrial ribosomal protein L10	20.84197352	0.0017	0.027768
NP_660298.2	MRPL10	mitochondrial ribosomal protein L12	2.125749708	0.000167	0.004961
NP_002940.2	MRPL12	mitochondrial ribosomal protein L14	1.246930861	2.05E-05	0.001034
NP_115487.2	MRPL14	mitochondrial ribosomal protein L16	0.78721493	0.000975	0.018312
NP_060310.1	MRPL16	mitochondrial ribosomal protein L17	1.040303677	0.000394	0.009306
NP_071344.1	MRPL17	mitochondrial ribosomal protein L19	1.177362424	2.78E-11	1.88E-08
NP_055578.2	MRPL19	mitochondrial ribosomal protein L22	1.952533129	0.003567	0.045504
NP_054899.2	MRPL22	mitochondrial ribosomal protein L37	1.625204792	1.05E-05	0.000604
NP_057575.2	MRPL37	mitochondrial ribosomal protein L38	1.639537175	3.09E-07	3.37E-05
NP_115867.2	MRPL38	mitochondrial ribosomal protein L39	1.860911054	1.39E-06	0.000117
NP_059142.2	MRPL39	mitochondrial ribosomal protein L4	1.141660382	0.000595	0.012804
NP_666499.1	MRPL4	mitochondrial ribosomal protein L40	1.58667978	0.003386	0.044718
NP_003767.2	MRPL40	mitochondrial ribosomal protein L41	1.685635314	0.000148	0.00456
NP_115866.1	MRPL41	mitochondrial ribosomal protein L43	1.507623245	9.46E-05	0.003107
NP_115488.2	MRPL43	mitochondrial ribosomal protein L44	1.313233802	6.03E-05	0.002215
NP_075066.1	MRPL44	mitochondrial ribosomal protein L46	1.201727649	0.000829	0.016203
NP_071446.2	MRPL46	mitochondrial ribosomal protein L47	1.253316938	0.000444	0.010149
NP_065142.2	MRPL47	mitochondrial ribosomal protein L48	1.314489494	5.83E-06	0.000358
NP_057139.1	MRPL48	mitochondrial ribosomal protein L49	1.091745841	0.000306	0.007671
NP_004918.1	MRPL49	mitochondrial ribosomal protein S10	1.207735868	0.004113	0.049489
NP_060611.2	MRPS10	mitochondrial ribosomal protein S14	1.311540717	1.16E-08	2.81E-06
NP_071383.1	MRPS14	mitochondrial ribosomal protein S14	1.108393289	1E-05	0.000583

NP_057118.1	MRPS2	mitochondrial ribosomal protein S2	1.721281062	0.00376	0.04744
NP_064576.1	MRPS22	mitochondrial ribosomal protein S22	1.667368136	1.1E-06	9.77E-05
NP_057154.2	MRPS23	mitochondrial ribosomal protein S23	1.686166276	0.000228	0.006358
NP_071942.1	MRPS25	mitochondrial ribosomal protein S25	1.102409689	0.001547	0.025817
NP_110438.1	MRPS26	mitochondrial ribosomal protein S26	1.031468386	0.000584	0.012649
NP_055899.2	MRPS27	mitochondrial ribosomal protein S27	1.510058968	1.64E-12	1.85E-09
NP_054737.1	MRPS28	mitochondrial ribosomal protein S28	1.255229473	2.63E-08	4.68E-06
NP_005821.2	MRPS31	mitochondrial ribosomal protein S31	1.392781781	0.002226	0.033299
NP_076425.1	MRPS34	mitochondrial ribosomal protein S34	1.17542536	2.24E-05	0.001099
NP_068593.2	MRPS35	mitochondrial ribosomal protein S35	1.413581473	2.78E-05	0.001324
NP_114108.1	MRPS5	mitochondrial ribosomal protein S5	2.212230307	7.14E-05	0.002485
NP_057055.2	MRPS7	mitochondrial ribosomal protein S7	1.10874506	0.000725	0.014769
NP_872578.1	MRPS9	mitochondrial ribosomal protein S9	1.981006242	4.51E-06	0.000293
NP_620132.1	MRRF	mitochondrial ribosome recycling factor	0.921605867	0.003923	0.048402
Older Resistance Training					
NP_004578.2	RRBP1	ribosome-binding protein 1	20.8031769	0.002159	0.044038
NP_733934.1	MRPL11	39S ribosomal protein L11, mitochondrial isoform b	2.345803022	9.60E-05	0.008532
NP_115867.2	MRPL38	39S ribosomal protein L38, mitochondrial	1.697080014	0.00015	0.009858
NP_003767.2	MRPL40	39S ribosomal protein L40, mitochondrial	1.522891707	0.000404	0.018395
NP_057118.1	MRPS2	28S ribosomal protein S2, mitochondrial	1.497722004	0.00035	0.017447
NP_071942.1	MRPS25	28S ribosomal protein S25, mitochondrial	1.466613292	0.000146	0.009855
NP_001186780.1	MRPS29	28S ribosomal protein S29, mitochondrial isoform 3	1.024101229	0.002623	0.04697
NP_001030178.1	RPL17	60S ribosomal protein L17 isoform a	0.951976294	0.001219	0.033703

Table S8, related to Figures 2 and 3: Exact p-values from 2-way ANOVA using Type 3 Estimates for change with training (Δ Training= post – pre) comparing main effects of Age, Group, and the Age x Group interaction. The p-values for Δ Training are adjusted for multiple comparisons using Tukey HSD and compared the change with training against 0. P-values of less than or equal to 0.05 were considered statistically different than 0. Mito FSR: Mitochondrial Fractional Synthesis Rate; Glucose R_d : Glucose Rate of Disappearance; RCR: Respiratory Control Ratio.

Variable	Δ Training								
	Age	Group	Age x Group	Young HIIT	Young RT	Young CT	Older HIIT	Older RT	Older CT
VO _{2 peak} (ml/min)	0.0569	0.0285	0.1527	<0.0001	0.0488	0.0001	0.0091	0.0528	0.0096
VO _{2 peak} (ml/kgBW/min)	0.1082	0.0015	0.0374	<0.0001	0.2458	<0.0001	0.0042	0.0596	0.0011
FFM (kg)	0.2767	0.0535	0.2453	0.0361	<0.0001	0.0058	0.0270	0.0042	0.0238
1RM/Leg FFM	0.8507	0.0015	0.8871	0.1601	<0.0001	0.0016	0.2737	<0.0001	0.0004
Mito FSR (%/hr)	0.0064	0.2681	0.1664	0.0244	0.2785	0.5691	0.0457	0.0206	0.0011
Glucose R_d (μ mol/kgFFM/min)	0.945	0.4303	0.5412	0.0226	0.0127	0.0423	0.0156	0.0032	0.5357
J O ₂ State 3 GMS (pmol O ₂ /μg mito/sec)	0.2732	0.5667	0.6929	0.5626	0.6981	0.7954	0.0571	0.0871	0.9102
J O ₂ State 3 GMS (pmol O ₂ /ml/sec)	0.8149	0.093	0.7263	0.0003	0.3933	0.0061	0.005	0.1462	0.0715
RCR (State 3/State 4)	0.8102	0.0614	0.2476	0.9253	0.1167	0.9244	0.1149	0.2233	0.0884
J H ₂ O ₂ State 3 GMS (pmol H ₂ O ₂ /mg mito/min)	0.0673	0.8562	0.6898	0.4593	0.1920	0.8384	0.2784	0.3130	0.4987
mtDNA copy (ND1/B2M)	0.2630	0.9780	0.7728	0.3942	0.0731	0.2031	0.0544	0.1251	0.0675

Supplemental Experimental Procedures

Overall study design

The study design was approved by the Mayo Clinic Institutional Review Board and registered under Clinical Trials #NCT01477164 and #NCT01738568 (clinicaltrials.gov). All participants were informed of study procedures and provided written consent. Eligible participants were randomized to either aerobic, resistance or combined groups. All groups had baseline testing that included an out-patient visit (for DEXA and $VO_{2\text{ peak}}$) and two in-patient studies (insulin clamp and biopsy). Participants then completed 12 weeks of training or sedentary period followed by repeated testing days. The combined group then performed 12 weeks of combined aerobic and resistance training followed by repeated testing days.

Screening

The study was advertised through television, radio, posted flyers, newspaper and word of mouth. Potential participants contacted the study team and completed a phone-screening questionnaire then eligible people were scheduled for an in-person screening visit. The screening visit including meeting with a study team member who described all procedures, then participants provided written consent. A fasting blood sample for complete blood count and urine sample for urinalysis were collected then general medical examination was performed. Participants met with a registered dietician to discuss food preferences for weighed-meals.

Inclusion/Exclusion Criteria

Participants were 18-30 years old or 65-80 years old. Exclusionary criteria included regular exercise routine (>20 minutes more than twice per week), cardiovascular disease, metabolic diseases (type 2 diabetes, fasting blood glucose >110 mg/dl and untreated hypo- or hyperthyroidism), renal disease, increased body mass index (>32 kg/m²), implanted metal devices (including joint replacements, stents, pacemaker, neurostimulators), pregnancy, smoking, history of blood clotting. Exclusionary medication included anticoagulants, insulin, corticosteroids, sulfonylureas, barbituates, PPAR γ agonists, β -blockers, sulfonylureas, insulin sensitizers, opiates and tricyclic antidepressants.

Out-patient visit

Approximately one week after screening, eligible participants reported to the Clinical Research Unit following an overnight fast (>10 hours) for resting energy expenditure (REE), body composition by dual-energy x-ray absorptiometry (DEXA) and peak aerobic capacity ($VO_{2\text{ peak}}$). First, participants lay in a quiet room with low lights for 30 minutes then REE was measured for 20 minutes using a ventilated hood (Parvo, Sandy, UT). Next, participants were analyzed for fat mass and fat free mass (FFM) by DEXA (Lunar). $VO_{2\text{ peak}}$ was determined on an electronically braked cycle ergometer using indirect calorimeter. Heart rate was measured with 12-lead electrocardiogram (Quintin) and manual blood pressures were collected. The incremental exercise test was 2-minute stages with the following workloads: Young Male 50W + 30W stages; Young Female 50W+ 20W stages; Older Male 50W+20W stages; Older Female 25W+20W stages. Participants were verbally encouraged throughout the test. The test was terminated when participants could not maintain a cadence of at least 60 revolutions per minute. $VO_{2\text{ peak}}$ was defined as reaching a rating of perceived exertion >17 according to Borg scale with respiratory exchange ratio >1.1 and within 10% of age predicted maximal heart rate.

Insulin Clamp

Insulin sensitivity was determined using a two-stage euglycemic clamp. Participants consumed 3-days of weighed meals (20% protein, 50% carbohydrates and 30% fat) to maintain body weight based on caloric requirement using Harris-Benedict equations. On the evening of the third day, participants reported to the Clinical Research Unit at 1730, consumed an evening meal at 1830 then were fasted overnight and throughout the insulin clamp. A catheter was inserted into an antecubital vein and maintained patent by saline infusion (30 ml/min). REE was measured for 20 minutes beginning at 0700 then a second catheter was inserted into an arm vein and a third into a dorsal hand vein on the contralateral arm. The hand was heated (120-131F) for arterialized blood sampling. Endogenous glucose production was traced using intravenous infusion of [6,6]-²H₂-glucose with a prime at 0500 (6 mg/kg FFM) followed by titrated infusion [3.6 (0500-0800), 2.52 (0800-0900), 1.8 (0900-1000), 1.368 (1000-1100) and 0.9 (1200-1400) mg/kg FFM/hour]. At 0800, regular insulin (Humulin) was infused (0.62 mU/kgFFM/min) along with somatostatin (0.093 mcg/kgFFM/min), glucagon (0.001 mcg/kgFFM/min) and human growth hormone (0.0047 mcg/kgFFM/min). Euglycemia (85-95mg/dl) was maintained by titrated infusion of 40% dextrose enriched (2%) with [6,6]-²H₂-glucose and saline was co-infused at an equal or greater rate to minimize phlebitis. At 1100, a second insulin infusion (1.68 mU/kg FFM/min) was added create a combined insulin infusion of 2.3 mU/kg FFM/min. Blood was sampled every 10 minutes and analyzed for glucose concentration in duplicate (\pm 3mg/dl for replicates).

Larger blood volumes were drawn hourly then every 15 minutes during the final steady state hour of low and high insulin infusions. The clamp was completed at 1400 then hormone infusions were tapered and discontinued at 1430. Participants consumed a meal and were discharged.

Muscle Biopsy

A muscle biopsy was collected 7-days after the insulin clamp. Participants repeated the 3-days of weighed meals and were admitted to the Clinical Research Unit of the evening of the third day. A light snack was provided at 2100 then participants remained fasting overnight. At 0700, 1000 and 1500 hours, biopsies (~350 mg) were collected from the vastus lateralis with analgesia by 2% lidocaine with sodium bicarbonate buffer. The 0700 sample was used for mitochondrial respiration and the 1000 hour sample for RNA sequencing.

Exercise training

Exercise training was performed for 12-weeks at the Dan Abraham Health Living Center at Mayo Clinic under the supervision of an exercise physiologist. Training intensity ranges were determined as heart rate at a percentage of $VO_{2\text{ peak}}$ and maintained ± 5 beat per minute using wireless monitors (Polar). Energy expenditure was determined for cycling and treadmill training from indirect calorimetry during the $VO_{2\text{ peak}}$ test and for resistance training from previously reported values (Phillips and Ziauraitis, 2003, 2004). Maximal strength was determined on leg press, lat pull down and chest press machines at baseline and following training for all groups. Participants warmed up for 10 minutes on bike, treadmill or elliptical machine, then were fitted to the machine and selected a weight to perform 10 repetitions. The weight was then increased and participants completed sets of up to 5 repetitions separated by a 1-minute rest. The highest weight that the participant could perform 1 repetition maximum (1RM) with good form was recorded.

High-intensity interval training consisted of 3 days per week of intervals on an electronically braked cycle ergometer (Monday, Wednesday and Friday) and 2 days per week on motorized treadmill walking (Tuesday and Thursday). The interval protocol was a 10-minute warm-up followed by 4 cycles of 4-minute high intervals ($> 90\%$) with 3-minute rest (pedaling at no load) then a 5-minute cool down. The time per session at high intensity was 16 minutes. The treadmill protocol was a self-selected walking pace (2-4 mph) with a 10-minute warm-up, 45 minutes at incline at $70\% VO_{2\text{ peak}}$ then a 5-minute cool down.

The resistance protocol was weight training for 60 minutes on 4-days per week of lower (Monday and Thursday) and upper body exercises (Tuesday and Friday). Participants were instructed on proper lifting technique and performed 8-12 repetitions per exercise with one-minute rest between sets. Participants completed two sets of each exercise for week 1, three sets for week 2, and four sets for weeks 3-12. Weights were increased when participants could perform 12 repetitions while maintaining good form. Lower body exercises were leg press, toe raise, lunge, abdominal crunch, leg extension and leg curl. Upper body exercises were chest press, lat pull down, incline chest press, seated row, lateral raise, biceps curl and triceps push down.

The combined protocol was 30 minutes of cycling 5-days per week (Monday through Friday) followed by 30 minutes of weight lifting. The cycling protocol was a five-minute warm-up, 20 minutes at $70\% VO_{2\text{ peak}}$, then 5 minutes of cool down. The weight lifting was a 4-day program with lower body (Monday and Thursday) and upper body exercises (Tuesday and Friday). Lower body exercises were leg press, abdominal crunch, leg extension and leg curls. Upper body exercises were chest press, lat pull down, triceps extensions and biceps curls.

Post-testing

The follow-up outpatient visits and maximal strength testing were performed on week 12 then participants continued training until beginning the metabolic meals. We were interested in determining the longer lasting effects of exercise training on insulin sensitivity and muscle mitochondrial function therefore follow-up in-patient studies were performed 72 hours after final training session (clamp performed 7 days after $VO_{2\text{ peak}}$). To avoid prolonged inactivity, participants performed 3 days of exercise training between in-patient study days followed by 3 days of inactivity during the metabolic meals.

Mitochondrial respiration

High-resolution respirometry was performed on mitochondria freshly isolated from the 0700 biopsy sample as previously described (Lanza and Nair, 2009). Approximately 100 mg of tissue was homogenized and mitochondria were separated using differential centrifugation. Mitochondria were added to a 2 ml chamber (Oxygraph-2K,

Oroboros) and allowed to equilibrate. Glutamate (10 mM) and malate (2 mM) were added to stimulate State 2 respiration specific to Complex I then ADP added at saturating concentrations (2.5 mM) to induce State 3 respiration of Complex I. Cytochrome-c was added to verify mitochondrial membrane integrity. Succinate (10 mM) was added to stimulate State 3 respiration through Complex I+II then rotenone (0.5 μ M) added to inhibit complex I for State 3 respiration specific to Complex II. State 4 respiration (Leak) was induced by addition of oligomycin (2 μ g/ μ l) then the proton gradient was dissipated by sequential titration of 0.05 mM carbonylcyanide-4-(trifluoromethoxy)-phenylhydrazone (FCCP) to induce uncoupled respiration. Protein content of isolated mitochondrial was determined using a commercially available kit (DC Protein Assay, Bio-Rad). Mitochondrial respiration was normalized to tissue wet weight (reflective of mitochondrial content) and mitochondrial protein (reflective of mitochondrial protein quality).

Muscle Tissue mRNA Sequencing

We used RNA-Seq technology to assess the muscle gene expression differences between various training groups. Total RNA was isolated from ~20 mg of the 1000 hour biopsy sample using a commercially available kit according to manufacturer's instructions (RNeasy Fibrous Tissue, Qiagen). Total RNA was eluted in 100 μ l of PCR grade water and concentration adjusted to 50 ng/ μ l using a spectrophotometer (Nanodrop, Thermo Scientific, Waltham, MA).

RNA libraries were prepared for sequencing using the TruSeq RNA Sample Prep Kit v2 (Illumina, San Diego, CA), following the manufacturer's recommendations. Briefly, poly-A mRNA was purified from 100 ng total RNA using oligo dT magnetic beads. Purified mRNA was fragmented at 95°C for 8 minutes and eluted from the beads. Double stranded cDNA was made using SuperScript III reverse transcriptase, random primers (Invitrogen, Carlsbad, CA) and DNA polymerase I and RNase H. The cDNA ends were repaired and an "A" base was added to the 3' ends. TruSeq paired end index DNA adaptors (Illumina, San Diego, CA) with a single "T" base overhang at the 3' end were ligated and the resulting constructs were purified using Agencourt AMPure SPRI beads (Beckman Coulter, Chaska, MN). Adapter-modified DNA fragments were enriched by 12 cycles of PCR using TruSeq PCR primers (Illumina, San Diego, CA). The concentration and size distribution of the libraries was determined on an Agilent Bioanalyzer DNA 1000 chip and Qubit fluorometry (Invitrogen, Carlsbad, CA).

Samples were divided into batches of eight and their indexed libraries were pooled at equimolar concentrations. Pooled library was loaded onto paired end flow cells at a concentration of 8.5pM to generate cluster densities of 700,000/mm² following the standard protocol for the Illumina cBot and cBot Paired-end cluster kit version 3. The flow cells were sequenced as 51X2 paired end reads on a HiSeq 2000 sequencer (Illumina, San Diego, CA) using TruSeq SBS sequencing kit version 3 (Illumina, San Diego, CA) and HCS version 2.0.12.0 data collection software. Base-calling is performed using Illumina's RTA version 1.17.21.3. On average, 56 million reads were generated for each sample. The RNA-Seq data were analyzed using the MAPRSeq (version 1.2.1) system for RNA-Sequencing data analysis.(Kalari et al., 2014)

Gene Expression Analysis

The total number of reads mapping to a gene was considered as a semi-quantitative measure of its abundance. We utilized edgeR software to perform differential expression analysis.(Robinson et al., 2010) Expression values of the genes present in each sample were normalized using its library depth. For each (age, exercise type) group, edgeR used generalized linear models, configured to take into account the paired design model, to detect differentially expressed genes. Genes with a FDR corrected p-value of ≤ 0.05 and an absolute log₂ fold change of ≥ 0.5 (where 0.0 signifies no change) were considered for further analysis.

mtDNA copy number

Total DNA was extracted using a kit (DNA mini, Qiagen) from the 1000 skeletal muscle biopsy sample and analyzed for mtDNA to nuclear DNA ratio as previously described (Lanza et al., 2012). qPCR was performed in 384 well clear plates with 20 μ l reaction volume. Amplification conditions were 10 minutes at 60°C followed by 40 cycles of denaturing (95°C for 15 s) and annealing (60°C for 60 s) using a ViiA7 thermocycler (Applied Biosystems). Samples were amplified with multiplex conditions for mtDNA and nDNA targets in triplicate. Each plate included a repeated control repeated on the plate (intra-assay control) and between plates (inter-assay control) along a no template control, and 7-point relative standard curve spanning 4 log dilutions. Primers and probes were commercially produced (Applied Biosystems) for ND1 (F: CCC GCC ACA TCT ACC ATC A, R: GAA GAG CGA TGG TGA GAG CTA AG, FAM® Probe: CCT CTA CAT CAC CGC CCC GA) and ND4 (F: CCC CAC CTT

GGC TAT CAT CA R: TAG GAA GTA TGT GCC TGC GTT C, FAM® Probe: CGA TGA GGC AAC CAG CCA GAA C) as mtDNA targets and β -2 microglobulin for nDNA (F: GTG CCT GAT ATA GCT TGA CAC AA, R: TCG GGA AAA GAC ACA TTA ATA TTG CCA, VIC® Probe: CCC CAA GTG AAA TAC C).

Infinium Methylation protocol

For the Infinium methylation protocol (Bibikova et al., 2009), 250ng of bisulfite modified DNA (1000ng input) is required the HumanMethylation450 BeadArray. Each probe is 75 bases long; 25 bases at the 5' end and are used for decoding (Gunderson et al Genome Res. 2004 May;14(5):870-7) and 50 bases are locus-specific. The oligonucleotides are immobilized on activated beads using a 5' amino group. The protocol involves isothermal whole genome amplification, followed by fragmentation and precipitation. These steps yield 50 μ g/ reaction and the average size after digestion to ~100-200 bases. Denatured products are hybridized to the BeadChip. The allele specific extension reaction, washing and staining are carried out in a TECAN Te-Flow Chamber. Stained BeadChips are then dried and imaged on an Illumina iScan reader. Following scanning on a BeadArray or iScan reader, intensity data are loaded into the GenomeStudio Methylation Module for analysis. Analysis includes control probes for assessing sample- independent and -dependent performance. The methylation status of the target CpG sites is determined by comparing the ratio of fluorescent signal from the methylated allele to the sum from the fluorescent signal from both methylated and unmethylated alleles. These values range from 0 (unmethylated) to 1 (methylated). Sample dependent controls include those for bisulfite conversion, allowing identification of samples with incomplete conversion. Positive (*SssI* treated DNA) and negative (WGA DNA) controls are included to determine whether there are any probes that should be excluded.

Raw methylation chip data was processed using GenomeStudio software (version 2011.1; Illumina, San Diego, CA). The software was configured to remove background using control probe data and normalize the spot intensities to account for chip-to-chip variation. GenomeStudio computed the methylation ratios (β) of all CpGs in each sample and exported them for processing in Partek Genomics Suite (version 6.13.0621; Partek Inc., St. Louis, MO). Samples were grouped in Partek according to age and exercise training regimen and any two groups of interest were compared using ANOVA models. Computed p-values were corrected using Benjamini-Hochberg method. For each CpG site, the software also computed the average beta values observed between the two groups. CpG sites that had a corrected p-value ≤ 0.05 and an absolute $\Delta\beta$ value of $\geq 0.05\%$ were considered as significant. CpG sites were filtered to retain candidates that were present within the known gene promoter regions (defined as $2000\text{bp} \leq \text{TSS} \leq 500\text{bp}$; TSS stands for transcription start site). The following pairwise group comparisons were performed: young vs. old at baseline, young pre-HIIT vs. post-HIIT, young pre-RT vs. post-RT, young pre-CT vs. post-CT, old pre-HIIT vs. post-HIIT, old pre-RT vs. post-RT, and old pre-CT vs. post-CT. A total of 3,874 promoter CpG sites were differentially methylated at baseline between young and old subjects. We did not observe any promoter CpG sites passing the above significant thresholds in any of the exercise training group comparisons.

Proteomics

A 25mg portion of the 1000 hour biopsy was powdered and homogenized at 1:10 dilution in buffer (50 mM Tris-HCl (pH 7.5), 5 mM MgCl₂, 250 mM sucrose, 0.5 mM EDTA). Homogenization was in a cooled bead mill (Beadruptor, Omni International) with 3x15s disruption protocol. Homogenates were then incubated on ice for ~10 minutes then spun at 720g for 10 minutes at 4°C, then supernatants transferred to a new tube and centrifuged at 16,600g for 20 minutes. Supernatant were collected for analysis. Protein estimation is performed using the Pierce 660 protein assay. Samples were diluted down to same concentration, and 40 μ g of muscle protein homogenate was loaded on to a 4-12% Bis-Tris Criterion Gel (345-0123, Bio-Rad). The gel was run at 80V constant with MES running buffer until the dye front reaches the bottom of the gel. The gel was then fixed and stained using coomassie. Each gel lane was cut into 8 segments that were incubated in 200 mM Tris 30 min prior to destaining with 50 mM Tris/40% acetonitrile for 1-2 hours. Segments were then dehydrated with 100% acetonitrile until gel pieces appeared opaque. Destaining was repeated three times followed by reduction with 50 mM TCEP for an hour, and alkylation with 25 mM IAA for an hour, dehydration with acetonitrile, hydration with 25 mM Tris for 10 minutes, and another dehydration prior to trypsin digest with 0.15 to 0.20 μ g trypsin in 20 mM Tris/0.0002% zwittergent 3-16 overnight at 37°C. Trypsin was inactivated and peptides were extracted by adding 3% trifluoroacetic acid to the digest for 20 minutes followed by the addition of acetonitrile for an additional 30 minutes. The supernatant was saved. Acetonitrile was added a second time to the gel segments which was added to the already saved supernatant. These peptide containing fractions were dried to completeness under vacuum and stored at -20°C.

Dried tryptic digests were reconstituted in 80 μ L sample buffer containing 0.2% formic acid, 0.1% TFA, 0.002% zwittergent 3-16, 0.2 fmol/ μ L Pierce retention time standards. A total of 10 μ L of the sample was used for analysis by nano-scale liquid chromatography interfaced to tandem mass spectrometry (nLC-MS/MS) using a Q-Exactive high resolution, accurate mass hybrid mass spectrometer. The Q-Exactive measured peptide molecular weights using 70,000 resolving power (FWHM, m/z 200) survey scans (MS1) followed by automated MS/MS experiments of the top 15 abundant precursor masses (charge states 2-4, inclusive). The peptides were separated by reversed phase nano-scale chromatography on a 100 μ m i.d. fused silica column packed in-house with 32 cm of Agilent Poroshell C18 stationary phase using a gradient of 2-45% B over 60 minutes with a mobile phase flow rate of 400 nL/min where mobile phase A was water, acetonitrile, and formic acid (98/2/0.2 by volume), and mobile phase B was composed of acetonitrile, isopropanol, water, and formic acid (80/10/10/0.2 by volume).

We utilized a peptide intensity-based label-free method for detecting protein and posttranslational modification differences between experimental groups. For this, MS/MS data were processed with MaxQuant software (version 1.5.1.2) configured to match the spectra against a composite protein sequence containing RefSeq human proteome (v58) and common contaminants. Reversed protein sequences were appended to the database for estimating peptide identification false discovery rates (FDRs.) MaxQuant used 20ppm peptide mass tolerance for first search and 4.5 ppm peptide mass tolerance for second search. The software was configured to derive semitryptic peptides from the database and identify the following PTMs as variable modifications: carbamidomethylation of cysteine, oxidation of methionine, oxidation of phenylalanine, oxidation of tryptophan, deamidation of asparagine, deamidation of glutamine, and n-terminal pyroglutamic acid. Peptide and protein identification results were filtered at 1% FDR. Non-redundant protein groups with at least two distinct peptide identifications were considered as present in the sample.

MaxQuant software reported protein group and peptide intensities for each sample. For protein differential expression, an in house R script processed the protein group intensity data. This script started by normalizing the sample level protein group intensities with the total ion current (TIC) detected for that sample. For each protein group, the normalized intensities observed in two groups of samples were modeled using a Gaussian-linked generalized linear model. An ANOVA test was used to detect the differentially expressed protein groups between pairs of experimental groups. Differential expression p-values were FDR corrected using Benjamini-Hochberg-Yekutieli procedure. Protein groups with an FDR \leq 0.05 and an absolute log₂ fold change of \geq 0.5 were considered as significantly differentially expressed. This process was previously described (Ayers-Ringler et al., 2016).

Peptide intensities were used to assess differential expression of specific PTMs between groups. For this, we obtained the ratio of modified to unmodified intensities (Mod/UnMod) for each peptide as previously described (Martin et al., 2016). These ratios were grouped by the PTM type (oxidation or deamidation) and experimental group. For each PTM type and experimental group, the difference between the post-exercise training and pre-exercise training Mod/UnMod ratios were computed for each peptide. The distribution of these delta Mod/UnMod ratios observed in each exercise training type was compared with those obtained from the sedentary group (SED) using a Mann-Whitney rank sum test. The resulting PTM results were summarized as average delta [Post-Pre] Mod/UnMod ratios observed for each exercise training type and a p-value comparing the observed distribution to that of SED group.

Supplemental References

- Ayers-Ringler, J.R., Oliveros, A., Qiu, Y., Lindberg, D.M., Hinton, D.J., Moore, R.M., Dasari, S., and Choi, D.S. (2016). Label-Free Proteomic Analysis of Protein Changes in the Striatum during Chronic Ethanol Use and Early Withdrawal. *Front Behav Neurosci* 10, 46.
- Bibikova, M., Le, J., Barnes, B., Saedinia-Melnyk, S., Zhou, L., Shen, R., and Gunderson, K.L. (2009). Genome-wide DNA methylation profiling using Infinium(R) assay. *Epigenomics* 1, 177-200.
- Kalari, K.R., Nair, A.A., Bhavsar, J.D., O'Brien, D.R., Davila, J.I., Bockol, M.A., Nie, J., Tang, X., Baheti, S., Doughty, J.B., et al. (2014). MAP-RSeq: Mayo Analysis Pipeline for RNA sequencing. *BMC Bioinformatics* 15, 224.
- Lanza, I.R., and Nair, K.S. (2009). Functional assessment of isolated mitochondria in vitro. *Methods in enzymology* 457, 349-372.
- Lanza, I.R., Zabielski, P., Klaus, K.A., Morse, D.M., Heppelmann, C.J., Bergen, H.R., 3rd, Dasari, S., Walrand, S., Short, K.R., Johnson, M.L., et al. (2012). Chronic caloric restriction preserves mitochondrial function in senescence without increasing mitochondrial biogenesis. *Cell metabolism* 16, 777-788.

Martin, D.R., Dutta, P., Mahajan, S., Varma, S., and Stevens, S.M., Jr. (2016). Structural and activity characterization of human PHPT1 after oxidative modification. *Sci Rep* 6, 23658.

Phillips, W.T., and Ziuraitis, J.R. (2003). Energy cost of the ACSM single-set resistance training protocol. *J Strength Cond Res* 17, 350-355.

Phillips, W.T., and Ziuraitis, J.R. (2004). Energy cost of single-set resistance training in older adults. *J Strength Cond Res* 18, 606-609.

Robinson, M.D., McCarthy, D.J., and Smyth, G.K. (2010). edgeR: a Bioconductor package for differential expression analysis of digital gene expression data. *Bioinformatics* 26, 139-140.